Supporting Information (SI) on

Macroscopic and Microscopic Investigation of U(VI) and Eu(III) Adsorption on Carbonaceous Nanofibers

Yubing Sun†,‡, Zhenyu Wu§, Xiangxue Wang†,‡, Congcong Ding†, Wencai Cheng†, Shuhong Yu§, Xiangke Wang‡,&,#*

† *Key Lab of New Thin Film Solar Cells, Institute of Plasma Physics, Chinese Academy of Sciences, P.O. Box 1126, Hefei, 230031, Anhui, P.R. China*

‡ *School of Environment and Chemical Engineering, North China Electric Power University, Beijing 102206, P.R. China*

§ *Division of Nanomaterials and Chemistry, Hefei National Laboratory for Physical Science at Microscale, Department of Chemistry, University of Science and Technology of China, Hefei, Anhui 230026*

& *School for Radiological and Interdisciplinary Sciences, Soochow University and Collaborative Innovation Center of Radiation Medicine of Jiangsu Higher Education Institutions, 215123, Suzhou, P.R. China*

Faculty of Science, King Abdulaziz University, Jeddah 21589, Saudi Arabia

*: Corresponding author. Phone: +86-10-61772890; Fax: +86-10-61772890; E-mail: xkwang@ncepu.edu.cn (X.K. Wang);

Submitted to **Environmental Science & Technology**

Supplemental Information, 19 pages with 6 Figures and 5 Tables

21 **List of Supplemental Figures**

22 **Figure S1**. The fitted results of pseudo-first-order and pseudo-second-order kinetic
23 models of U(VI) and Eu(III) sorption on the CNFs.

24 **Figure S2.** Gran plots of the CNFs titration at 0.01mol/L $NaClO_4$, V_0 = 40 mL, *m*/v =
25 0.16 g/L and T = 298 K.

26 **Figure S3**. The relative distribution of radionuclides as a function of pH in aqueous
27 solutions, C_0 = 10.0 mg/L, I = 0.01 mol/L $NaClO_4$, T = 298 K.

28 **Figure S4.** The amount of $UO_2(OH)_2$ (A) and $Eu(OH)_3$(s) (B) under atmospheric CO_2,
29 C_0 = 10 mg/L, T = 298 K.

30 **Figure S5**. The k^2-weighted U L_{III}-edge EXAFS spectra of the reference and samples,
31 m/V = 0.16 g/L, $C_{U(VI)}$ = 10.0 mg/L, I = 0.01 mol/L $NaClO_4$, T = 298 K.

32 **Figure S6**. k^2-weighted Eu L_{III}-edge EXAFS spectra (A) and the corresponding
33 Fourier Transforms (B) of the reference samples and selected adsorption samples at
34 pH 4.5 and 7.0, respectively, m/V = 0.16 g/L, $C_{Eu(III)}$ = 10.0 g/L, I = 0.01 mol/L
35 $NaClO_4$, T = 298 K.

36

Table List

Table S1. The parameters of pseudo-first-order and pseudo-second-order kinetic model of U(VI) and Eu(III) sorption on the CNFs.

Table S2. The equilibrium constants of U(VI) and Eu(III) species in aqueous solution at 298 K.

Table S3. The binding energy of the CNFs after Eu(III)/U(VI) adsorption and desorption.

Table S4. The deconvolution of C 1s of the CNFs after radionuclides adsorption.

Table S5. EXAFS results of reference samples and Eu(III) adsorbed on the CNFs at Eu L_{III}-Edge, $T = 298$ K, $I = 0.01$ mol·L^{-1} $NaClO_4$.

Synthesis of Carbonaceous Nanofibers (CNFs). The CNFs were prepared by the template- directed hydrothermal carbonization (HTC) process.[S1] Briefly, 30 mL of acetone was added into 10 mL of the prepared Te nanowire solution to precipitate the product before centrifuging at 6000 rpm, which was then dispersed into 80 mL of glucose solution (5.0 g of glucose) under vigorous stirring for 15 min. Hydrothermal treatment of the mixed solution at 160 ºC for different times could result in Te@C nanocables with various diameters. Pure CNFs could be obtained by removal of Te templates by chemical etching in an acidic H_2O_2 solution.

Preparation of IR, XPS, XANES and EXAFS Samples.

The samples for IR and XPS analysis were prepared as followed procedures: 3.0 mL of 0.1 mol/L $NaClO_4$ solution and 15 mL of 20.0 mg/L U(VI) or Eu(III) were added into 50 mL polycarbonate tubes, and then 12 mL of 0.4 g/L the CNF solution were added into the aforementioned solution. The pH values of suspension were adjusted to be 4.5 by adding negligible volume of 0.1-5.0 mol/L $HClO_4$ or NaOH solution. Then the suspension was agitated on a shaker for a reaction time of 24 h. The solid and liquid phases were separated by centrifugation at 7104 ×*g* for 30 min. The samples for IR and XPS analysis were obtained by drying them in vacuum oven overnight. For samples of XPS analysis after desorption (CNFs_U(d) and CNFs_ Eu(d)), 15 mL of the aforementioned supernate after centrifugation was removed and then 15 mL of 0.02 mol/L $NaClO_4$ solution was added. The pH values of suspension were adjusted to be 4.5 by adding negligible volume of 0.1-5.0 mol/L $HClO_4$ or NaOH solution. Then suspension was agitated on a shaker for a reaction time of 24 h. The solid and

70 liquid phases were separated by centrifugation at 7104 ×*g* for 30 min. The powder
71 was obtained by freeze drying it overnight.
72 The samples for XANES and EXAFS analysis of Eu(III)- and U(VI)-bearing CNFs at
73 different pH and initial concentrations were prepared in the glove box filled with
74 nitrogen gas (< 1 ppm CO_2) to eliminate the effect of atmospheric CO_2 on the fitting
75 of U/Eu-C shell of CNFs. Briefly, the CNFs with 0.01 mol/L $NaClO_4$ were weighted
76 into 250 mL flask bottles and then Milli-Q water (boiled then bubbled with Ar gas)
77 was added and pre-equilibrated for 24 h. The CO_2-free $Eu(NO_3)_3$ or $UO_2(NO_3)_2$
78 solutions were slowly dropwise added under vigorous stirring conditions. Then the
79 suspensions were adjusted to pH 4.5 or 7.0 by using negligible volume 0.01-1.0 mol/L
80 $HClO_4$ or NaOH solution. Samples were then gently agitated on a shaker for 24 h.
81 The solid phase was separated from liquid phase by centrifugation at 7104 × *g* for 30
82 min and then through 0.22-μm membrane filters. The wet pastes of Eu(III)- and
83 U(VI)- bearing CNFs were mounted in Teflon sample holders with Kapton tape.
84 **Analysis of EXAFS data.** Uranium and europium L_{III}-edge EXAFS spectra were
85 measured at Shanghai Synchrotron Radiation Facility (SSRF, Shanghai, China) using
86 Si(111) double-crystal monochromator. The spectra of all samples were collected in
87 fluorescence mode with high-throughput 30-element solid-state Ge detector. For
88 XANES analysis, the data of reference samples ($U^{IV}O_2$(s) and $U^{VI}O_2^{2+}$) were derived
89 from our previous studies.[S2] EXAFS spectra were extracted from the subtraction of
90 background and the correction of energy for raw EXAFS data. The extracted EXAFS
91 spectra of Eu(III) and U(VI) were Fourier transformed (FT) using the *k* range of

2.0-10.0 and 2.8-11.5 $Å^{-1}$, respectively. The values of R for Eu(III) and U(VI) were set in the range of 0-6.0 and 0-9.0 Å, respectively. The k^2-weighted EXAFS data were analyzed using Athena and Artemis interfaces to IFFEFIT 7.0 software.[S3] The paths of U-O_{ax}, U-O_{eq}, U-C and U-U shells were fitted from the crystal structures of schoepite ($(UO_2)_8O_2(OH)_2 \cdot 12H_2O$) and Rutherfordine ($UO_2CO_3$),[S4,S5] whereas the Eu-O, Eu-Eu and Eu-C shells were fitted from the crystal structures of $Eu(OH)_3$[S6] and $[Eu(\mu\text{-}CH_3COO)(CH_3COO)_2\ (H_2O)_2]_2 \cdot 4H_2O$.[S7]

Batch Adsorption Kinetics and Isotherms. For adsorption kinetics, 0.6 mL of 0.1 mol/L $NaClO_4$ solution and 3.0 mL of 20.0 mg/L U(VI) or Eu(III) solution were added into 10 mL polycarbonate tubes. The pH of the suspension was adjusted to 4.5 and then the suspension was agitated on a shaker for different reaction times ranging from 2.0 to 240 min. For adsorption isotherms, 0.6 mL of 0.1 mol/L $NaClO_4$ solution and 3.0 mL of 1.0-30.0 mg/L U(VI) or Eu(III) solution were added to the 10 mL polycarbonate tubes. The pH of the suspension was adjusted to 4.5, and the suspension was then agitated on a shaker for a reaction time of 24 h. The solid and liquid phases were separated by centrifugation at 7104 ×*g* for 30 min.

The calculation of amount of reduction of U(VI) to U(IV). The amount of reduction of U(VI) to U(IV) was calculated by the change in the energies of adsorption edge of XANES spectra. A linear combination of the samples was fitted by using the two references spectra of $U^{VI}O_2^{2+}$ and $U^{IV}O_2$ (s). Therefore, the amount of reduction of U(VI) to U(IV) can be calculated as Eqn. (S1):

$$\text{Reduction (\%)} = \frac{100 \times (E_{0\_U(VI)} - E_{0\_sample})}{E_{0\_U(VI)} - E_{0\_U(IV)}} \qquad \text{(S1)}$$

where $E_{0\_U(VI)}$, E_{0_sample} and $E_{0\_U(IV)}$ referred to the energies of adsorption edge (E_0 values) of $U^{VI}O_2^{2+}$, CNFs_U(a1) pH 7.0 and $U^{IV}O_2$ (s), respectively. The values of $E_{0\_U(VI)}$, E_{0_sample} and $E_{0\_U(IV)}$ were 17178.503, 17177.980 and 17177.029 eV, respectively. Therefore, the percentage of reduction of U(VI) to U(IV) was calculated to 35.48 %.

Adsorption Kinetics. The pseudo-first-order and pseudo-second-order kinetic models can be described by Eqns. S2 and S3, respectively:

$$\ln(q_e - q_t) = \ln q_e - k_f \times t \quad \text{(S2)}$$

$$\frac{t}{q_t} = \frac{1}{k_s \times q_e^2} + \frac{t}{q_e} \quad \text{(S3)}$$

where q_e and q_t (mg/g) are the amount of radionuclides adsorbed at equilibrium and at time t, respectively. k_f and k_s are the pseudo-first order and pseudo-second order kinetic rate constant, respectively. The fitted results and the corresponding kinetic parameters are shown in Figure S1 and Table S1, respectively.

Table S1. The parameters of pseudo-first-order and pseudo-second-order kinetic model of U(VI) and Eu(III) sorption on the CNFs

Adsorbates	Pseudo-first-order			Pseudo-second-order		
	qe (mg/g)	kf (min^{-1})	R^2	qe (mg/g)	ks (g/(mg·min))	R^2
U(VI)	139.35	0.044	0.927	1000	5.00×10^{-4}	0.999
Eu(III)	303.69	0.0060	0.735	1000	7.65×10^{-5}	0.999

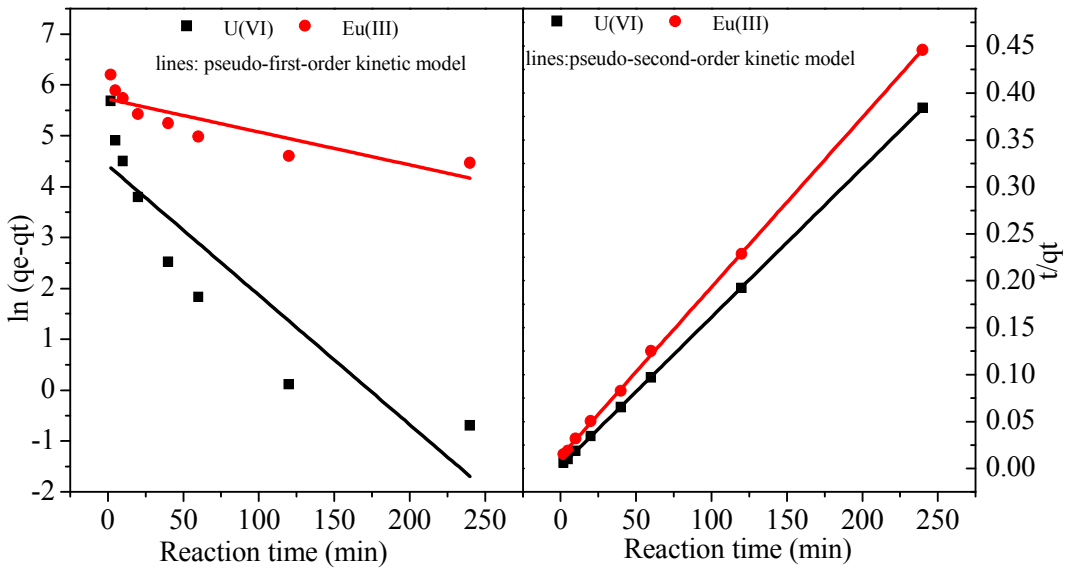

Figure S1. The fitted results of pseudo-first-order and pseudo-second-order kinetic models of U(VI) and Eu(III) sorption on the CNFs

Calculation of Surface Site Concentration. The surface site concentration of the CNFs was calculated according to data of acid-base titration. The acid-base titration of the CNFs at 0.01 mol/L $NaClO_4$ solution was performed at 298 K with a DL50 Automatic Titrator (Mettler Toledo, Switzerland). Briefly, 40 mL of 0.16 g/L the CNFs with 0.01 mol·L^{-1} $NaClO_4$ background electrolyte was purged with argon gas (< 1 ppm CO_2) for 60 min under vigorous stirring to exclude atmospheric CO_2(g). The initial suspensions were adjusted to pH 3.0 by adding 0.1 mol/L HNO_3 solution gradually. The base titrations were conducted to pH 11.0 with 0.01 mol/L NaOH titrant at a variable increment (0.002 to 0.02 mL) under the dynamic mode and the equilibration time conditions. The values of Gran function (G) at acid and base side can be calculated by *Eqns*. S4 and S5, respectively:[S8]

At acid side: $G_a = (V_0 + V_a + V_b) \times 10^{-pH} \times 100$ (S4)

At base side: $G_b = (V_0 + V_a + V_b) \times 10^{-(13.8-pH)} \times 100$ (S5)

where G_a and G_b are the Gran functions at the acid and base sides, respectively; V_0 is the initial volume of the suspension. V_a and V_b represent the total volume of acid added and base added at different titration points, respectively. The linear regression analysis of Gran plots at acid side (V_{eb1}) and at base side (V_{eb2}) can be considered as the neutralization with excess H^+ cations. As shown in Figure S3, the value of V_{eb1} and V_{eb2} were calculated to be 0.55 and 2.2 mL at 0.01 mol/L $NaClO_4$ solution.

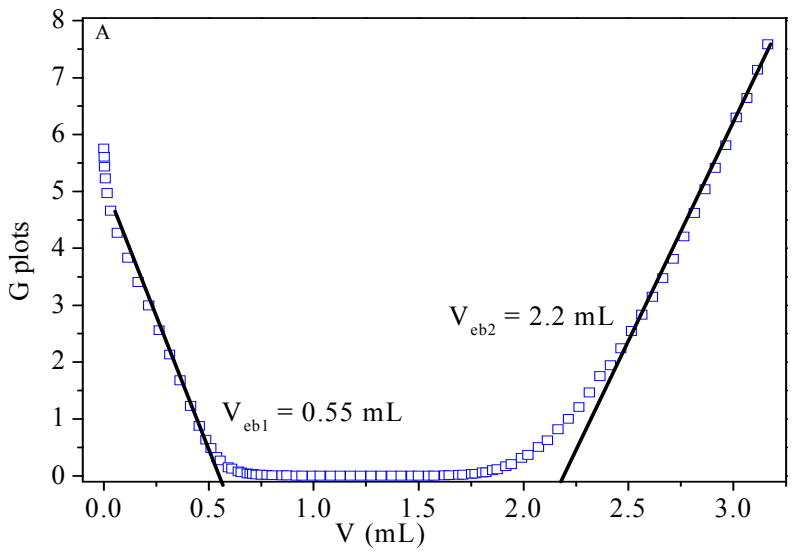

Figure S2. Gran plots of the CNF titration at 0.01mol/L $NaClO_4$, V_0 = 40 mL, m/v = 0.16 g/L and T = 298 K.

The total surface site concentration of the CNFs per solid weight (H_s, mmol/g) calculated from the two equivalence points on the Gran plot (V_{eb1} and V_{eb2}) is defined by the Eqn. (S6):[S9]

$$H_s = \frac{(V_{eb2} - V_{eb1}) \times C_b}{m_s} \qquad \text{(S6)}$$

where C_b and m_s refer to the concentration of NaOH (0.01 mol/L) and mass of the CNFs (0.0064 g), respectively. Therefore, the total surface site concentration of the CNFs was calculated to be 2.578 mmol/g.

Distribution of radionuclides in aqueous solutions. The distribution of U(VI) and Eu(III) in aqueous solutions were calculation by visual MINTEQ mode (Figure S3).[S10]

Table S2. The equilibrium constants of U(VI) and Eu(III) species in aqueous solution

Reactions	Log K	Ref.
U(VI)		
$UO_2^{2+} + H_2O = UO_2OH^+ + H^+$	-5.20	(S11)
$UO_2^{2+} + 2H_2O = UO_2(OH)_2 + 2H^+$	-11.50	(S11)
$UO_2^{2+} + 3H_2O = UO_2(OH)_3^- + 3H^+$	-20.00	(S11)
$UO_2^{2+} + 4H_2O = UO_2(OH)_4^{2-} + 4H^+$	-33.00	(S11)
$UO_2^{2+} + CO_3^{2-} = UO_2CO_3$ (s)	9.68	(S11)
$UO_2^{2+} + 2CO_3^{2-} = UO_2(CO_3)_2^{2-}$	16.94	(S11)
$UO_2^{2+} + 3CO_3^{2-} = UO_2(CO_3)_3^{4-}$	21.60	(S11)
Eu(III)		
$Eu^{3+} + H_2O = EuOH^{2+} + H^+$	-7.64	(S12)
$Eu^{3+} + 2H_2O = Eu(OH)_2^+ + 2H^+$	-15.10	(S12)
$Eu^{3+} + 3H_2O = Eu(OH)_3 + 3H^+$	-23.70	(S12)
$Eu^{3+} + 4H_2O = Eu(OH)_4^- + H^+$	-36.20	(S12)
$Eu^{3+} + CO_3^{2-} = EuCO_3^+$	8.10	(S12)
$Eu^{3+} + 2CO_3^{2-} = Eu(CO_3)_2^-$	12.10	(S12)

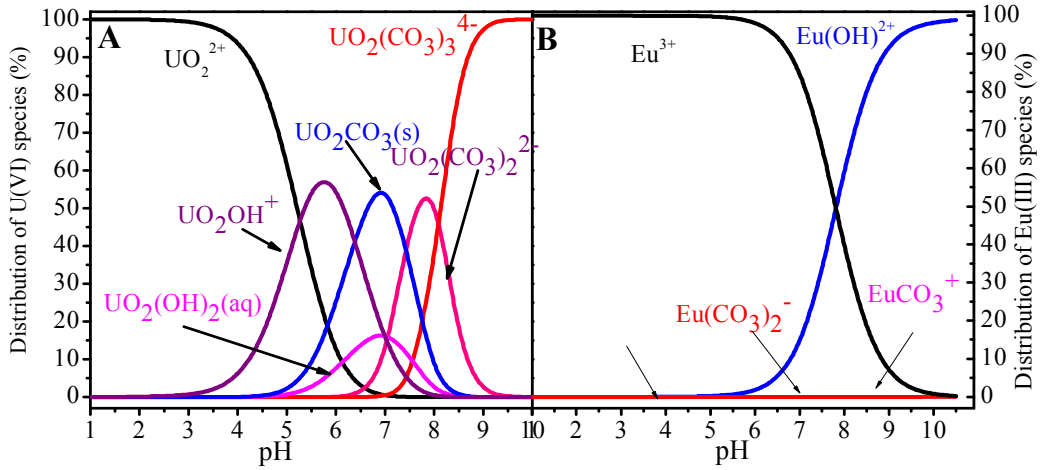

Figure S3. The relative distribution of radionuclides as a function of pH in aqueous solutions, C_0 = 10.0 mg/L, $P_{CO_2} = 10^{-3.5}$ atm, I = 0.01 mol·L^{-1} $NaClO_4$, T = 298 K.

Calculation of precipitate. The amount of schoepite and $Eu(OH)_3(s)$ under atmospheric CO_2 was derived from the previous study.

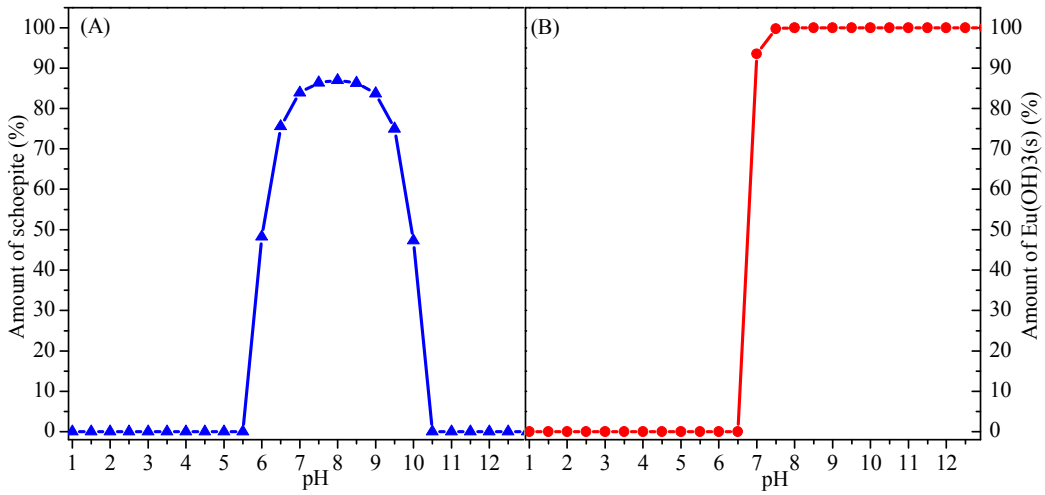

Figure S4. The amount of schoepite (A) and $Eu(OH)_3(s)$ (B) under atmospheric CO_2, C_0 = 10 mg/L, T = 298 K.

Adsorption Isotherms. The Langmuir and Freundlich models can be expressed by Eqns. (S7) and (S8), respectively:

$$Q_e = \frac{q_m \times K_L \times C_e}{1 + K_L \times C_e} \quad \text{(S7)}$$

$$Q_e = K_F \times C_e^{1/n} \quad \text{(S8)}$$

where C_e (mg/L) and Q_e (mg/g) refer to the equilibrium solute concentration and the amount of adsorbate adsorbed per unit mass of adsorbent, respectively. K_L (L/mg) and K_F ($(mg^{1-n}L^n g^{-1})$) are the equilibrium constants of Langmuir and Frenudlich models, respectively. q_m (mg/g) represents the maximum adsorption capacity.

XPS analysis. The difference in binding energies of C 1s and O 1s of the CNFs before and after U(VI) and Eu(III) desorption was summarized in Table S3.

185 **Table S3**. The binding energy of the CNFs after Eu(III)/U(VI) adsorption and

186 desorption.

	C (eV)	O (eV)	Radionuclide (eV)
CNFs	284.79	531.93	NA[c]
CNFs_Eu(a)[a]	284.80	532.37	1135.39
CNFs_Eu(d)[b]	284.81	532.04	NA
CNFs_U(a)	284.74	532.98	335.3
CNFs_U(d)	284.24	532.29	NA

187 [a] Adsorption of Eu(III) on CNFs; [b] Desorption of Eu(III) on CNFs; [c] no analysis;

188 **Table S4**. The deconvolution of C 1s of the CNFs after radionuclides adsorption.

Samples	Functional groups	Binding energy (eV)	Relative ratios (%)
CNFs	C-C	284.70	64.28
	C-O	286.02	20.98
	C=O	287.80	9.050
	C(O)O	289.00	5.690
CNFs_U(a)	C-C	284.72	68.51
	C-O	286.24	17.61
	C=O	287.60	7.060
	C(O)O	288.86	6.820
CNFs_Eu(a)	C-C	284.72	56.19
	C-O	286.06	25.93
	C=O	287.31	5.670
	C(O)O	288.51	12.21

189 **EXAFS Spectra Analysis of U(VI) Samples.** Figure S5 showed the k^2-weighted U

190 L_{III}-edge EXAFS spectra of the reference (UO_2^{2+}, schoepite) and samples

191 (CNFs_U(a2) pH 4.5, CNFs_U(a1) pH 4.5 and CNFs_U(a1) pH 7.0). The EXAFS

192 spectra of UO_2^{2+} species showed a distinct cyclic evolution, whereas a different

193 feature for $UO_2(OH)_2$ precipitate was observed at $\kappa > 6$ Å^{-1} due to the existence of

194 U-U back scattering. As shown in Figure S6, the similar EXAFS spectra features were

195 observed for CNFs_U(a1) pH 4.5 and CNFs_U(a1) pH 7.0, whereas the FT features

of CNFs_U(a2) pH 4.5 were significantly different from those of CNFs_U(a1) pH 4.5 and CNFs_U(a1) pH 7.0.

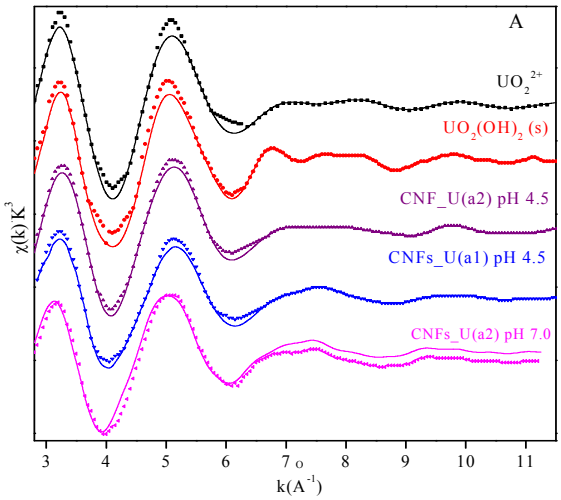

Figure S5. The k^2-weighted U L_{III}-edge EXAFS spectra of the reference and samples, m/V = 0.16 g/L, $C_{U(VI)}$ = 10.0 mg/L, I = 0.01 mol/L $NaClO_4$, T = 298 K.

EXAFS Spectra Analysis of Eu(III) Samples. Figure S6A and S6B showed the k^2-weighted europium EXAFS spectra and the corresponding Fourier transform (FT) data of reference samples and CNFs_Eu pH 4.5 and CNFs_Eu pH 7.0, respectively. The position of absorption line at ~6983 eV indicated that Eu was trivalent in all samples in terms of X-ray absorption near edge structure spectra.[S13]

For aqueous Eu(III) ions, a single wave frequency of monotonically decreasing amplitude was observed at $k > 3$ Å^{-1} (Figure S6A), which was attributed to a single ordered coordination shell.[S14] The EXAFS spectra for crystalline $Eu(OH)_3$ displayed evident frequencies compared to aqueous Eu(III) ions. The difference was not only attributed to multiple backscattering paths in the first coordination shell, but also can be related to the presence of higher atomic shells.[S15] Compared to reference samples, the broaden oscillation at $k \sim 6.5$ Å^{-1} for CNFs_Eu pH 4.5 and CNFs_Eu pH 7.0 was

due to the formation of inner-sphere surface complexes.[S13]

As shown in Figure S6B, FT features at near 2.0 Å for all samples were related to the contributions from oxygen atoms of the nearest coordination shell. High amplitude contributions at R ~3.6 Å for crystalline $Eu(OH)_3$ originated mainly from next-nearest Eu backscattering shells.[S15] Only weak contribution at ~ 3.1 Å for crystalline $Eu(OH)_3$, aqueous Eu(III) ions may originate either from multiple backscattering paths within the first coordination shell or from single backscattering paths from second and more distant hydration spheres. The results are quite in good agreement with the results of Eu(III) interaction with calcium silicate hydrates.[S15] FT features displayed the slightly difference between aqueous Eu(III) ions and CNFs_Eu pH 4.5 and CNFs_Eu pH 7.0, but the oscillations at k ~ 6.5 $Å^{-1}$ for CNFs_Eu pH 4.5 and CNFs_Eu pH 7.0 were wider than aqueous Eu(III) ions. FT features of obtained for Eu(III) adsorbed on CNFs_Eu pH 7.0 looks similar to crystalline $Eu(OH)_3$, but difference somewhat is observed at R ~ 4.2 Å. The fit to the EXAFS data was simultaneously done for reference samples and CNFs_Eu pH 4.5 and CNFs_Eu pH 7.0 (dash lines at Figure S7A). The structural parameters derived from EXAFS analyses were summarized in Table S5. The $R_{Eu\text{-}O}$ value of ~2.45 Å for CNFs_Eu pH 4.5 and CNFs_Eu pH 7.0 was an average bond distance composed of Eu-O contribution, the hydration shell Eu-OH_2 and the excessive carboxylate groups Eu-O (CNFs) contribution on Eu(III) adsorption on the CNFs.[S14-S16] The coordination number of first coordination shell (Eu-O path) decreases from ~6.69 to ~6.02 with pH increasing from 4.5 to 7.0, which indicated that the Eu(III) was coordinated with a hydration sphere of ~7 O in the first

coordination shell on CNFs_Eu pH 4.5 and with ~ 6 O in the first coordination shell at pH 7.0. Attempts to include the Eu-C sphere contribution to the EXAFS data for CNFs_Eu pH 7.0 suggested the formation the inner-sphere surface complexes. Results of EXAFS analysis suggested that the interaction mechanism between Eu(III) and the CNFs was determined from mononuclear monodentate complexes to binuclear bidentate surface complexes with increasing pH values.

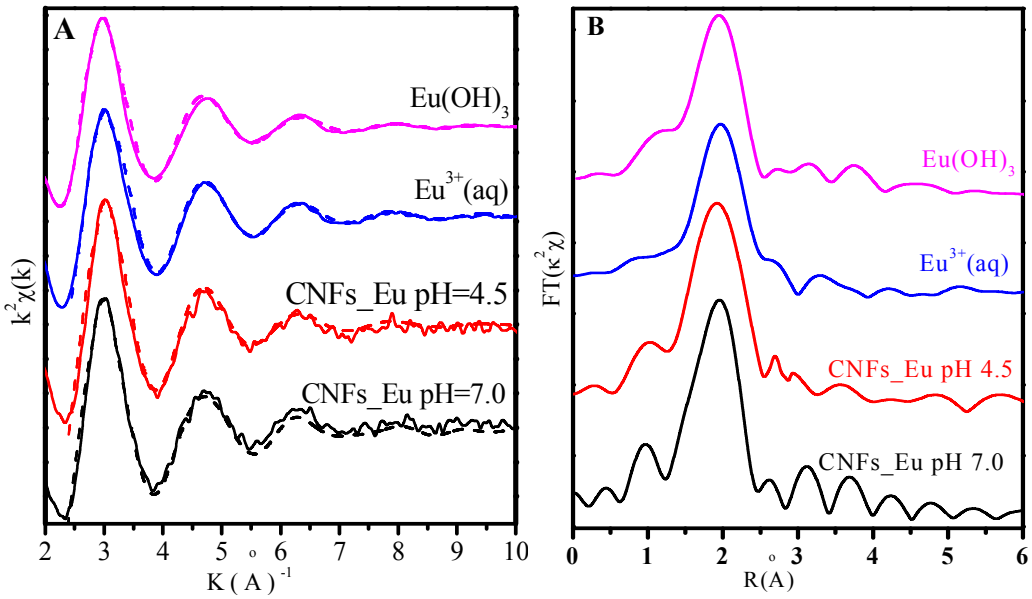

Figure S6. k^2-weighted Eu L_{III}-edge EXAFS spectra (A) and the corresponding Fourier Transforms (B) of the reference samples and selected adsorption samples, respectively, m/V = 0.16 g/L, $C_{Eu(III)}$ = 10.0 mg/L, I = 0.01 mol/L $NaClO_4$, T = 298 K.

Table S5. EXAFS results of reference samples and Eu(III) adsorbed on the CNFs at Eu L_{III}-Edge, T= 298 K, I=0.01 mol·L^{-1} $NaClO_4$

Sample	shell	R(Å)[a]	N[b]	σ^2(Å ^{2})[c]
$Eu(OH)_3$	Eu-O	2.404(8)	9.08(0)	0.0015(8)
	Eu-Eu	3.648(9)	1.91(0)	0.0055(0)
Eu(aq)	Eu-O	2.423(1)	8.47(4)	0.0067(3)
CNFs at pH 4.5	Eu-O	2.412(8)	6.68(0)	0.0060(0)
	Eu-C	2.316(9)	4.01(9)	0.0060(0)
CNFs at pH 7.0	Eu-O	2.407(5)	6.03(4)	0.0030(0)
	Eu-C	2.311(0)	4.42(0)	0.0030(0)
	Eu-Eu	3.531(2)	2.35(8)	0.0030(0)

[a]R: the bond distance. [b]N: coordination numbers of neighbors. [c]σ^2: the Debye-Waller factor.

References

(S1) Qian, H. S.; Yu, S. H.; Luo, L. B.; Gong, J. Y.; Fei, L. F.; Liu, X. M. Synthesis of uniform Te@carbon-rich composite nanocables with photoluminescence properties and carbonaceous nanofibers by the hydrothermal carbonization of glucose. *Chem. Mater.* **2006**, *18*, 2102-2108.

(S2) Sun, Y. B.; Ding, C. C.; Cheng W. C.; Wang, X. K. Simultaneous adsorption and reduction of U(VI) on reduced graphene oxide- supported nanoscale zerovalent iron. *J. Hazard. Mater.* **2014**, *280*, 399-408.

(S3) Ravel, B.; Newville, M. ATHENA, ARTEMIS, HEPHAESTUS: data analysis for X-ray absorption spectroscopy using IFEFFIT. *J. Synchrot. Radiat.* **2005**, *12*, 537-541.

(S4) Finch, R. J.; Cooper, M. A.; Hawthorne, F. C.; Ewing, R. C. The crystal structure of schoepite, $[(UO_2)_8O_8(OH)_{12}.\ 12H_2O$. *Can. Mineral.* **1996**, *34*, 1071-1088.

(S5) Finch, R. J.; Cooper, M. A.; Hawthorne, F. C.; Ewing, R. C. Refinement of the crystal structure of rutherfordine. *Can. Mineral.* **1999**, *37*, 929-938.

(S6) Mullica, D. F.; Milligan, W. O.; Beall, G. W. Crystal structures of $Pr(OH)_3$, $Eu(OH)_3$ and $Tm(OH)_3$. *J. Inorg. Chem.* **1979**, *41*, 525-532.

(S7) Yang, Y; Luo, L; Thomas, C. W. M. Crystal structure of [Eu(*u*-CH_3COO-O) $(CH_3COO)_2(H_2O)_2]\cdot 4H_2O$. *J. Struct. Chem.* **1988**, *7*, 1-5.

(S8) Chen, C. L.; Hu, J.; Xu, D.; Tan, X. L.; Meng, Y. D.; Wang, X. K. Surface complexation modeling of Sr(II) and Eu(III) adsorption onto oxidized multiwall carbon nanotubes. *J. Colloid Interface Sci.* **2008**, *323*, 33-41.

(S9) Frini-Srasra, N.; Srasar, E. Determination of acid-base properties of HCl acid activated palygorskite by potentiometric titration. *Surf. Eng. Appl. Electrochem.* **2008**, *44*, 401-409.

(S10) Gustafsson, J. P. Visual MINTEQ ver. 2.53. KTH, Department of Land and Water Resources Engineering. Stockholm; 2006.

(S11) Davis, J. A.; Meece, D. E.; Kohler, M.; Curtis, G. P. Approaches to surface complexation modeling of uranium(VI) adsorption on aquifer sediments. *Geochim. Cosmochim. Acta* **2004**, *68*, 3621-3641.

(S12) Thoenen, T.; Hummel, W.; Berner, U.; Curti, E. *The PSI/Nagra Chemical Thermodynamic Database 12/07*, Paul Scherrer Institut, Villigen PSI, Switzerland, 2014.

(S13) Stumpf, T.; Curtis, H.; Walther, C.; Dardenne, K.; Ufer, K.; Fanghanel, T. Incorporation of Eu(III) into hydrotalcite: A TRLFS and EXAFS study. *Environ. Sci.*

Technol. **2007**, *41*, 3186-3191.

(S14) Janot, N.; Benedetti, M. F.; Reiller, P. E. Colloidal alpha–Al_2O_3, Europium (III) and humic substances interactions: A macroscopic and spectroscopic study. *Environ. Sci. Technol.* **2011**, *45*, 3224-3230.

(S15) Schlegel, M. L.; Pointeau, I.; Coreau, N.; Reiller, P. Mechanism of europium retention by calcium silicate hydrates: an EXAFS study. *Environ. Sci. Technol.* **2004**, *38*, 4423-4431.

(S16) Fan, Q. H.; Tan, X. L.; Li, J. X.; Wang, X. K.; Wu, W. S.; Montavon, G. Sorption of Eu(III) on attapulgite studied by batch, XPS and EXAFS techniques. *Environ. Sci. Technol.* **2009**, *43*, 5776-5782.